Mid-infrared photothermal heterodyne spectroscopy in a liquid crystal using a quantum cascade laser

Alket Mërtiri, Thomas Jeys, Vladimir Liberman, M. K. Hong, Jerome Mertz, Hatice Altug, and Shyamsunder Erramilli

Articles you may be interested in

Mid-infrared quantitative spectroscopy by comb-referencing of a quantum-cascade-laser: Application to the CO2 spectrum at 4.3m
Appl. Phys. Lett. **99**, 251107 (2011); 10.1063/1.3671081

High-resolution heterodyne spectroscopy using a tunable quantum cascade laser around 3.5 THz
Appl. Phys. Lett. **98**, 231109 (2011); 10.1063/1.3599518

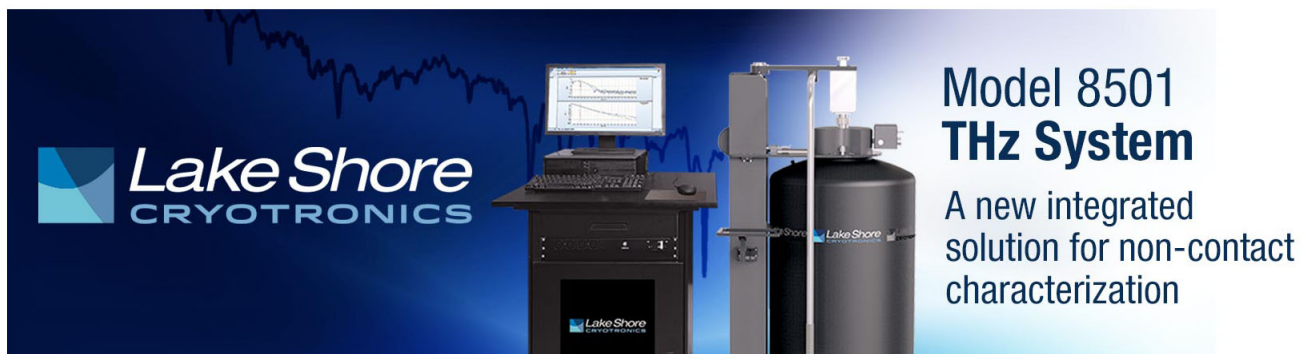3.4 THz heterodyne receiver using a hot electron bolometer and a distributed feedback quantum cascade laser
J. Appl. Phys. **104**, 113106 (2008); 10.1063/1.3032354

Ground-based prototype quantum cascade laser heterodyne radiometer for atmospheric studies
Rev. Sci. Instrum. **78**, 073107 (2007); 10.1063/1.2753141

InP-based quantum cascade detectors in the mid-infrared
Appl. Phys. Lett. **88**, 241118 (2006); 10.1063/1.2210088

Mid-infrared photothermal heterodyne spectroscopy in a liquid crystal using a quantum cascade laser

Alket Mërtiri,[1,2] Thomas Jeys,[3] Vladimir Liberman,[3] M. K. Hong,[2,4] Jerome Mertz,[2,5] Hatice Altug,[2,6] and Shyamsunder Erramilli[2,4,5,a)]

[1]*Division of Material Science and Engineering, Boston University, Boston, Massachusetts 02215, USA*
[2]*Photonics Center, 8 St. Mary's St, Boston, Massachusetts 02215, USA*
[3]*Lincoln Laboratory, Massachusetts Institute of Technology, Lexington, Massachusetts 02420, USA*
[4]*Department of Physics, Boston University, Boston, Massachusetts 02215, USA*
[5]*Department of Biomedical Engineering, Boston University, Boston, Massachusetts 02215, USA*
[6]*Department of Electrical and Computer Engineering, Boston University, Boston, Massachusetts 02215, USA*

We report a technique to measure the mid-infrared photothermal response induced by a tunable quantum cascade laser in the neat liquid crystal 4-octyl-4′-cyanobiphenyl (8CB), without any intercalated dye. Heterodyne detection using a Ti:sapphire laser of the response in the solid, smectic, nematic and isotropic liquid crystal phases allows direct detection of a weak mid-infrared normal mode absorption using an inexpensive photodetector. At high pump power in the nematic phase, we observe an interesting peak splitting in the photothermal response. Tunable lasers that can access still stronger modes will facilitate photothermal heterodyne mid-infrared vibrational spectroscopy. © 2012 American Institute of Physics. [http://dx.doi.org/10.1063/1.4737942]

Photothermal spectroscopy has rapidly emerged as the most sensitive label-free optical spectroscopic method, rivaling even fluorescence spectroscopy. The method has been shown to be remarkably sensitive in the visible region of the spectrum with reports of yoctomole sensitivity, eventually culminating in the observation of single molecule response[1,2,28] at room temperature. This unexpected sensitivity has led to rapid development of photothermal methods in the visible region, both for spectroscopy[3–5] and for imaging nanoparticles and organelles with high signal-to-noise ratio.[6,7]

Extension of the photothermal technique to the mid-infrared region is particularly attractive because the presence of a large number of characteristic normal modes of molecules in the so-called "fingerprint" region of the electromagnetic spectrum allows for spectroscopy and imaging without requiring a perturbing label. The standard instrument of choice for vibrational infrared spectroscopy remains Fourier transform infrared spectroscopy (FTIR) using cryogenically cooled detectors along with a ∼1200 K Globar blackbody source. But the lack of table-top stable high brightness sources and a fundamental quantum limit on the detectivity of broadband cryogenic mid-infrared detectors has translated to a lack of progress: the state-of-the-art[8] has not advanced significantly in several decades. Detection of the absorption of infrared radiation is still performed using narrow band-gap cryogenically cooled detectors made of indium antimonide (InSb) or mercury-cadmium-telluride (MCT),[8] which both are intrinsically less sensitive than the best available visible photodetectors. With the advent of tunable quantum cascade lasers (QCLs) as table-top high brightness sources, there is now hope of a rapid transformation in the field of mid-infrared spectroscopy.[9,10] The spectral brightness of these table-top QCL sources actually can exceed that of synchro-trons and other large relativistic electron-accelerator-based sources.[1] Very recently, Farahi et al.[11] have demonstrated a homodyne photothermal spectroscopy method for remote sensing. Our work[12] shows that photothermal heterodyne detection of absorption of a tunable Quantum Cascade laser source promises to out-perform conventional FTIR spectrometers.

In photothermal spectroscopy,[13] a modulated pump laser beam that is tuned to a selected absorption spectral band in a sample causes change in the scattered intensity of a probe beam. The probe beam typically differs in color, corresponding to a wavelength far from the absorption resonance. The observed probe scattering signal arises primarily from modulated change in the refractive index Δn due to localized heating by the pump beam. The change in the refractive index can be detected by measuring the modulated scattering intensity, which is proportional to $(\Delta n)^2$ in homodyne detection. The signal is phase locked to the modulation frequency of the pump beam using a conventional photodetector and a lock-in amplifier. We use photothermal heterodyne[7] spectroscopy to study the room-temperature liquid crystal 4-Octyl-4′-Cyanobiphenyl (8CB). Cyanobiphenyls form a well-studied class of liquid crystals, with rich phase behavior[14,15] characterized by strong vibrational infrared absorption bands in the fingerprint region.[16] Our pump beam is a mid-IR QCL that can be tuned to a molecular normal mode that lies within the wavelength tuning range of the laser of $1830\,cm^{-1}$ to $1990\,cm^{-1}$. The probe beam is provided by a Ti:sapphire laser operating in CW mode at 800 nm. The 4-Octyl-4′-Cyanobiphenyl (8CB) liquid crystal sample was sandwiched between cleaned calcium fluoride (CaF_2) windows with $50\,\mu m$ Mylar spacer. In the absence of rubbing or surface coating the molecular alignment is homogeneous, with no preferred direction at either CaF_2 window substrate. Observation of the sample with visible light under crossed polarizers did not show homeotropic alignment of the sample as a whole. The FTIR absorbance

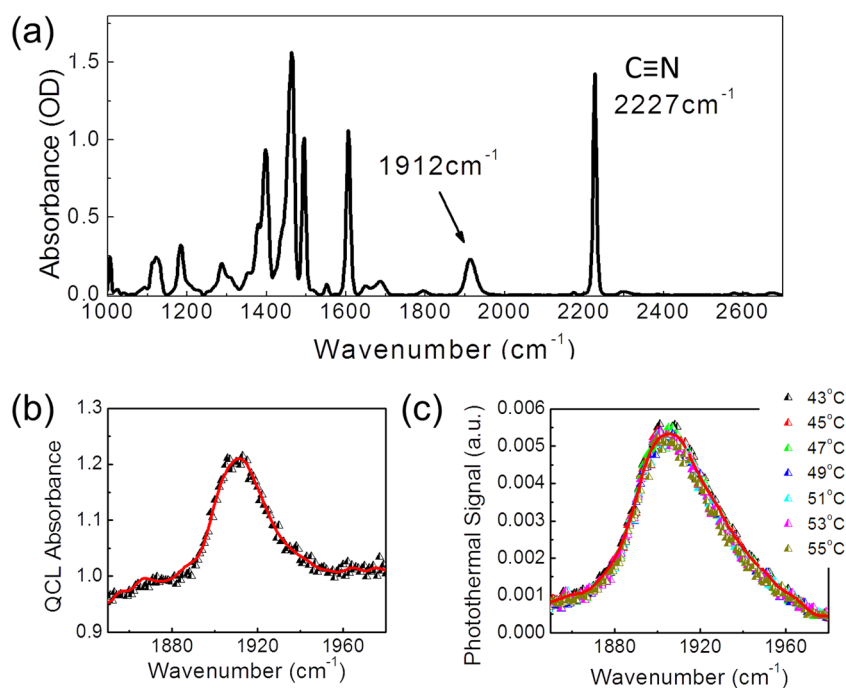a)Author to whom correspondence should be addressed. Electronic mail: shyam@bu.edu.

FIG. 1. (a) FTIR absorption spectra at a spectral resolution of $4\,cm^{-1}$ of $50\,\mu m$ thick 8CB liquid crystal sample showing the sharp C-N stretch band at $2227\,cm^{-1}$ and the weak combination band at $1912\,cm^{-1}$. (b) Absorbance of 8CB measured with liquid-nitrogen cooled InSb detector and QCL as the mid-infrared source, with a spectral resolution of $1\,cm^{-1}$ at the indicated temperature. (c) Photothermal response in the isotropic phase, using a Si photodetector.

spectrum as shown in Fig. 1(a) has a sharp C-N stretch band at $2227\,cm^{-1}$. A weak combination band, thought to arise from out-of-plane CH vibrations,[17] is shown in Fig. 1(b) centered at $1912\,cm^{-1}$ and lies within the tuning range of the laser with a molar extinction coefficient of $14.9\,M^{-1}\,cm^{-1}$. Fig. 1(c) shows the corresponding photothermal response on the same sample. The signal shown is the probe response from an inexpensive silicon photodiode plotted as a function of the mid-infrared QLC frequency. The photothermal signal, due to the weak mid-infrared combination mode, could be observed in the smectic, nematic, and isotropic phases of the 8CB liquid crystal.

The experimental setup is shown in Fig. 2(a), illustrating a collinear two-photon pump-probe spectroscopy with the use of QCL as the pump heating beam with a center wavelength and Ti:sapphire as the probe beam. A mid IR QCL beam at $5.23\,\mu m$ serves as the heating beam and a cw beam at 800 nm serves as a probe. The QCL beam is modulated with a mechanical chopper at 20 Hz frequency. Alternatively, the QCL may be operated in pulse mode, modulated up to 100 kHz with a maximum duty cycle of 5%. The two beams are collinearly combined using a dichroic mirror (DM) and focused coaxially into the sample by a zinc-selenide (ZnSe) focusing objective (NA = 0.25). The mid-IR QCL Gaussian beam is focused into the sample with a beam waist diameter of $22\,\mu m \pm 3\,\mu m$. The Ti:sapphire probe has a beam waist diameter of $16\,\mu m \pm 3\,\mu m$. The transmitted beams are collected by a ZnSe lens. The pump and probe beams are separated using a second beamsplitter. They are focused onto an InSb liquid nitrogen-cooled detector and a Si-photodetector for pump and probe beam measurements, respectively. This set-up allows for comparison between direct mid-infrared detection and heterodyne photothermal detection in the same sample under identical conditions (Fig. 1).

8CB liquid crystal undergoes well-known phase transitions, from smectic-A phase to nematic phase at 306.5 K and from the nematic phase to isotropic phase at 313.5 K.[18–20] A

representation of the molecular orientations for each phase studied is shown in Fig. 2(b). In the smectic-A phase, the molecular long axis is perpendicular to the plane of layers. In the nematic phase the molecules align along an average direction. Above 313.5 K, 8CB liquid crystal is in the isotropic phase, where the molecules do not have a specific orientation.

The QCL mid IR laser beam was tuned at the absorption peak of the sample and the output power was varied from 40 mW to 65 mW. Losses at the beamsplitters and coupling optics resulted in an estimated incident intensity on the sample of $\sim 1.2 \times 10^4\,W/cm^2$. The probe beam power was set at
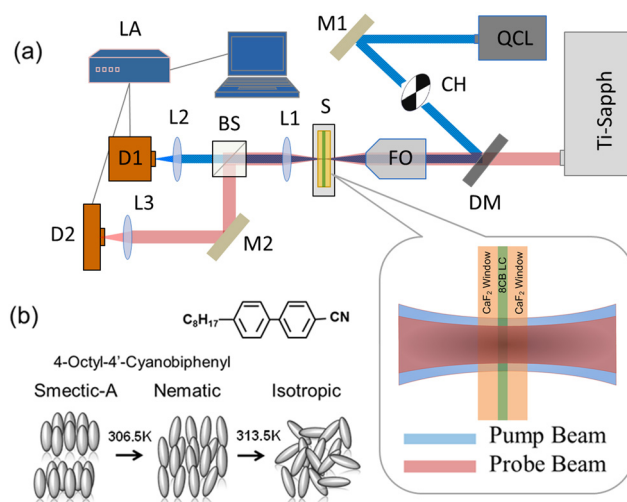

FIG. 2. Experimental setup for photothermal detection and 8CB liquid crystal properties. (a) Heating QCL pump beam and Ti:sapphire probe beam are spatially co-aligned with the dichroic mirror and focused onto the sample with ZnSe focusing objective. M-mirror, CH-mechanical chopper, DM-dichroic mirror, FO-focusing objective, S-sample, HC-temperature controlled heating cell, L-lens, BS-beamsplitter, D-detector, LA-lock-in amplifier. (b) 8CB liquid crystal phases. Smectic-A phase; the molecular axis are perpendicular to the plane of layers. Nematic phase; the molecules on average are aligned in a specific direction. Isotropic phase; molecules do not have a particular direction.

100 mW in the cw mode, with the estimated probe intensity at the sample of $\sim 2 \times 10^4\,\mathrm{W/cm^2}$. The base temperature of the sample is controlled using a circulating water bath, and it can be varied for the initial temperature of the sample to be set in any of the desired liquid crystal phases. When the 8CB sample is illuminated with the QCL mid-IR source, a local transient temperature jump is induced at the focused spot leading to the photothermal response shown in Fig. 3(a) for all the phases. Prior studies have demonstrated the utility of the photothermal effect in dye-doped liquid crystals[21] and shown important guest-host interactions between the dye and the liquid crystals.[22] A recent paper[23] used visible light absorption gold nanoparticles to show enhanced photothermal response due to thermotropic transitions in a 5CB liquid crystal sample. Our work reports on the direct photothermal excitation of mid-infrared vibrational normal modes in the liquid crystal molecules.

Figure 3 shows the mid-infrared photothermal response in the solid, smectic-A, nematic and isotropic phases. The initial temperature on the sample was controlled with a liquid chiller/heater and the temperature was varied from 13 °C to 55 °C. The mid-infrared photothermal response increases linearly as the 8CB sample base temperature is increased from 13 °C to 35 °C as shown in Figs. 3(b) and 3(c). In the solid phase, Fig. 3(b), and in the smectic-A phase, Fig. 3(c), the photothermal signal increased linearly and the peak shape was unchanged as we increased the temperature. The photothermal response also increased linearly in the nematic

phase, but it remained constant in the isotropic phase as shown in Fig. 3(e). As we approached the isotropic region, however, the shape of the photothermal signal changed. Here we observed peak splitting effect, which is shown in Fig. 3(d). The photothermal response for all the studied phases is shown in Fig. 3(a).

Apparent peak splitting in *nonlinear* photothermal and photoacoustic spectroscopy of nanoparticles in the visible region previously has been reported by Zharov,[24] where the effect was attributed to reduced scattering from "nanobubbles" caused by laser heating. Optical scattering from thermally generated clusters[24] reduces the photothermal response in the nonlinear regime. Such a mechanism for peak splitting is expected to hold for mid-infrared photothermal spectroscopy as well. This reduced signal is expected to coincide with the peak of the infrared pump absorption, i.e. at $1912\,\mathrm{cm^{-1}}$, as shown in Fig 3(d). The microscopic mechanism for bubble or cluster generation, and the scattering cross-section, varies from sample to sample. At high input power, a central volume near the focal spot of the liquid crystal sample in the nematic phase may be photothermally excited into the isotropic phase, resulting in the formation of clusters of the isotropic phase in a cooler nematic environment. Alternate mechanisms may include nonlinear variation in the dielectric response, from dimerization[25] or a change in the order parameter.[26] Refinement of a quantitative nonlinear model will allow for the microscopic mechanism behind the observed peak splitting to be clarified. The observed peak
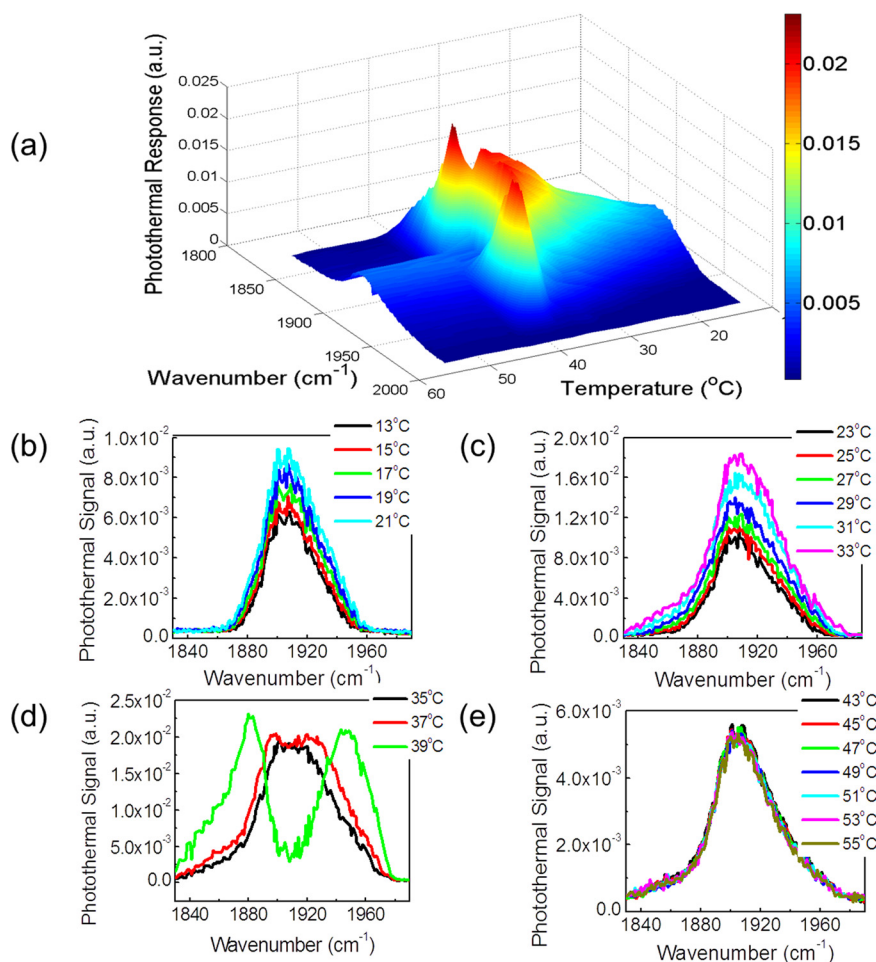

FIG. 3. Photothermal response on 8CB liquid crystal sample. (a) Photothermal response of the 50 μm thick 8CB liquid crystal as a function of temperature for all the measured phases. (b) Photothermal response in the solid phase, T = 13 °C, 15 °C, 17 °C, 19 °C, and 21 °C. (c) Photothermal response in the smectic-A phase, T = 23 °C, 25 °C, 27 °C, 29 °C, 31 °C, 33 °C. (d) Photothermal response in the nematic phase, T = 35 °C, 37 °C, and 39 °C. (e) Photothermal response in the isotropic phase, T = 43 °C to 55 °C.
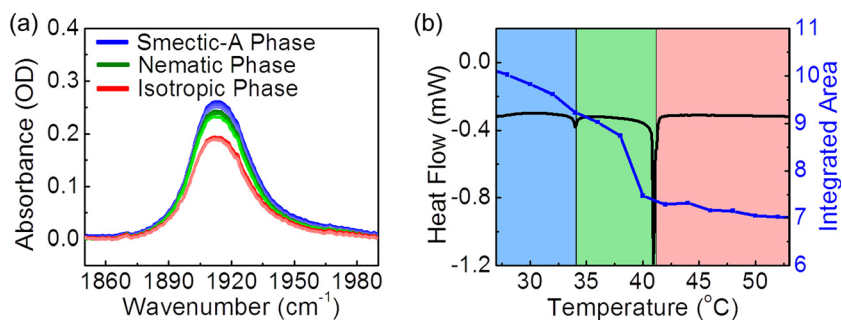
FIG. 4. (a) Dependence of 8CB liquid crystal absorbance on the sample temperature, by FTIR spectroscopy at 4 cm⁻¹ resolution. The smectic-A absorptions peaks are shown in blue, the nematic phase in green and the isotropic phase in red. (b) Integrated area under the absorbance peaks varying the temperature on the 8CB liquid crystal sample. Smectic-A phase (blue region), Nematic phase (green region) and Isotropic phase (red region). DSC measurement on 8CB liquid crystal. Endothermic peaks show the phase transition temperature from Smectic-A (blue region) to Nematic (green region) at 33.7 °C and Nematic to isotropic (red region) at 40.8 °C.

splitting phenomenon shares some general aspects of spectral hole burning,[27] but the approach is qualitatively different. In classical hole burning, the imaginary part of the dielectric function at the probe frequency is altered (i.e., reduced absorption). In our case the real part of the dielectric response at the probe frequency, related to the refractive index, is altered. In support of this hypothesis, we note below that the spectrum measured by the cryogenic infrared detector does *not* show peak splitting; only the scattered photothermal response does. At high power, in the nonlinear regime near phase transitions, the photothermal response shows features not observed in linear FTIR spectroscopy.

Detailed simulations of this effect will be reported elsewhere. To verify that the signal is indeed due to the photothermal response, we measured the FTIR absorption by varying the temperature on the 8CB liquid crystal sample as shown in Fig. 4(a). We looked at the combination band in the IR absorption spectra at 1912 cm⁻¹. As we increased the temperature well in the isotropic phase, we observed no peak splitting effect. Within each phase, the area under the absorbance peaks decreased as we increased the sample temperature as shown in Fig. 4(b). This decrease in integrated area arises most likely from a change in molecular orientation correlated to the order parameter, but additional studies are needed to quantify the correlation. We observed a change in slope at the nematic-isotropic phase transition boundary, consistent with the differential scanning calorimetry (DSC) measurements. At high laser power incident on a sample poised just below the phase transition temperature, the photothermal signals can be extremely sensitive and nonlinear, leading to observed differences from linear FTIR spectroscopy. Taken together, our work suggests that linear photothermal infrared heterodyne detection can map infrared spectral features consistent with FTIR within a given phase.

In conclusion, we report the detection of a mid-infrared spectrum using photothermal spectroscopy. As an illustration, we report on the observation of a mid-infrared photothermal signal in a liquid crystal sample near room temperature. The method allows for detection of mid-infrared absorption without using expensive cryogenic detectors.

[1]G. L. Carr, P. Dumas, C. J. Hirschmugl, and G. P. Williams, "Nuovo Cimento Della Societa Italiana Di Fisica D-Condens Matter At. Mol.," Chem. Phys. Fluids Plasmas, Biophys. **20**(4), 375–395 (1998).
[2]A. M. Armani, R. P. Kulkarni, S. E. Fraser, R. C. Flagan, and K. J. Vahala, Science **317**(5839), 783–787 (2007).
[3]D. Lasne, G. A. Blab, F. De Giorgi, F. Ichas, B. Lounis, and L. Cognet, Opt Express **15**(21), 14184–14193 (2007).
[4]S. Lu, Appl. Phys. Lett. **96**(11), 113701 (2010).
[5]L. Cognet, C. Tardin, D. Boyer, D. Choquet, P. Tamarat and B. Lounis, Proc. Natl. Acad. Sci. **100**(20), 11350–11355 (2003).
[6]D. Boyer, P. Tamarat, A. Maali, B. Lounis, and M. Orrit, Science **297**(5584), 1160–1163 (2002).
[7]S. Berciaud, D. Lasne, G. A. Blab, L. Cognet, and B. Lounis, Phys. Rev. B **73**(4), 045424 (2006).
[8]P. R. Griffiths and J. A. De Haseth, *Fourier Transform Infrared Spectrometry*, 2nd ed. (Wiley, New York, 2007).
[9]J. Faist, F. Capasso, D. L. Sivco, C. Sirtori, A. L. Hutchinson, and A. Y. Cho, Science **264**(5158), 553–556 (1994).
[10]F. Capasso, C. Gmachl, R. Paiella, A. Tredicucci, A. L. Hutchinson, D. L. Sivco, J. N. Baillargeon, A. Y. Cho, and H. C. Liu, IEEE J. Sel. Top. Quantum Electron. **6**(6), 931–947 (2000).
[11]R. H. Farahi, A. Passian, L. Tetard, and T. Thundat, J. Phys. D: Appl. Phys. **45**, 125101 (2012).
[12]A. Mertiri, M. K. Hong, J. Mertz, H. Altug, and S. Erramilli, APS March Meeting Bulletin Y1.00011, 2012.
[13]S. E. Bialkowski, *Photothermal Spectroscopy Methods for Chemical Analysis* (Wiley, 1996).
[14]S. Kumar, L. Chen, and V. Surendranath, Phys. Rev. Lett. **67**(3), 322–325 (1991).
[15]S. Kumar and S.-W. Kang, in *Encyclopedia of Condensed Matter*, edited by G. Bassani, G. Liedl and P. Wyder (Elsevier Ltd., Oxford, UK, 2005), Vol. 3, pp. 111–120.
[16]M. Thomas, Vib. Spectrosc. **24**(1), 137–146 (2000).
[17]L. Frunza, H. Kosslick, U. Bentrup, I. Pitsch, R. Fricke, S. Frunza, and A. Schonhals, J. Mol. Struct. **651**, 341–347 (2003).
[18]D. Davidov, C. R. Safinya, M. Kaplan, S. S. Dana, R. Schaetzing, R. J. Birgeneau, and J. D. Litster, Phys. Rev. B **19**(3), 1657 (1979).
[19]Z. Kutnjak, S. Kralj, G. Lahajnar, and S. Zumer, Fluid Phase Equilib. **222–223**(0), 275–281 (2004).
[20]J. Thoen, H. Marynissen, and W. Van Dael, Phys. Rev. A **26**(5), 2886 (1982).
[21]C. S. Yelleswarapu, S. R. Kothapalli, F. J. Aranda, D. V. G. L. N. Rao, Y. R. Vaillancourt, and B. R. Kimball, Appl. Phys. Lett. **89**, 2111161–2111163 (2006).
[22]T. V. Truong, L. Xu, and Y. R. Shen, Phys. Rev. Lett. **90** 193902 (2003).
[23]A. N. G. Parra-Vasquez, L. Oudjedi, L. Cognet, and B. Lounis, J. Phys. Chem. **3**, 1400–1403 (2012).
[24]V. P. Zharov, Nature Photon. **5**(2), 110–116 (2011).
[25]L. M. Babkov, I. I. Gnatyuk, and S. V. Trukhachev, J. Mol. Struct. **744–747**, 425–432 (2005).
[26]S. Chandrasekhar, *Liquid Crystals* (Cambridge University Press, 1992).
[27]S. Mukamel, *Principles of Nonlinear Spectroscopy* (Oxford University Press, New York, 1995).
[28]A. Gaiduk, M. Yorulmaz, P. V. Ruijgrok, and M. Orrit, Science **330**(6002), 353–356 (2010).